Supporting Information

Torsion effect of imide ring on the performance of transparent polyimide films with methyl-substituted phenylenediamine

Huanyu Lei[1,2], Feng Bao[1,2], Weifeng Peng[1,2], Luhao Qiu[1,2], Bingyu Zou [1,2], Mingjun Huang[1,2*]*

[1] South China Advanced Institute for Soft Matter Science and Technology, School of Emergent Soft Matter, South China University of Technology, Guangzhou 510640, China.

[2] Guangdong Provincial Key Laboratory of Functional and Intelligent Hybrid Materials and Devices, South China University of Technology, Guangzhou 510640, China.

*Corresponding author

E-mail address:
huangmj25@scut.edu.cn (M.H.)

fbao@scut.edu.cn (F.B.)

This file includes:

1. **Supplementary Figure S1-S9**
2. **Supplementary Table S1-6**

1. Supplementary Figure

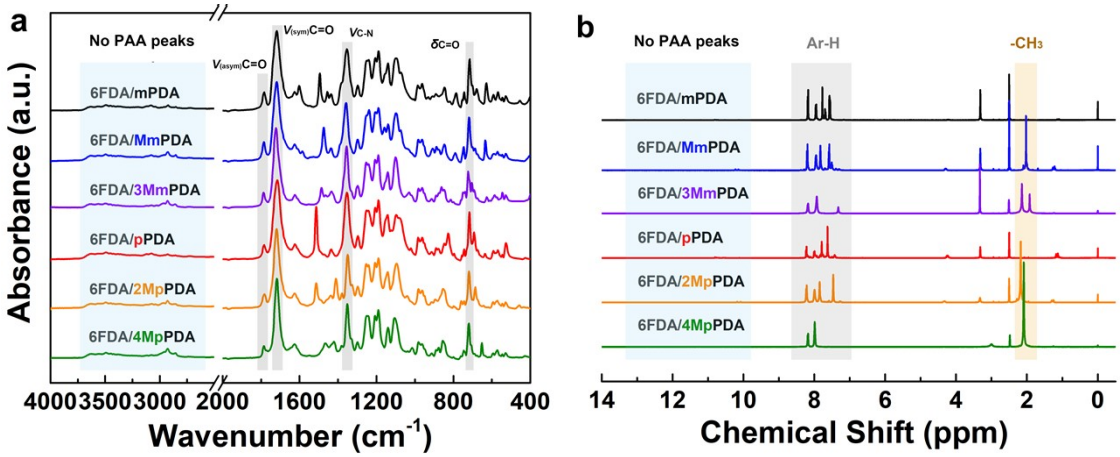

Fig S1 (a) ATR-FTIR and (b) ^{1}H NMR spectra of CPI films. For ^{1}H NMR testing, all CPIs were dissolved in DMSO-d_6 containing TMS as reference, and only 6FDA/4MpPDA CPI was characterized at high temperature (100 °C) for completed solvation.

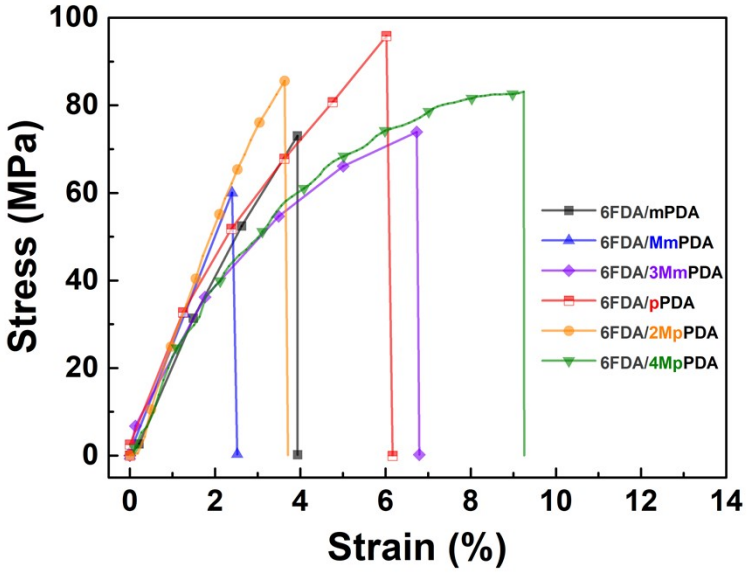

Fig S2 Mechanical properties of CPI films.

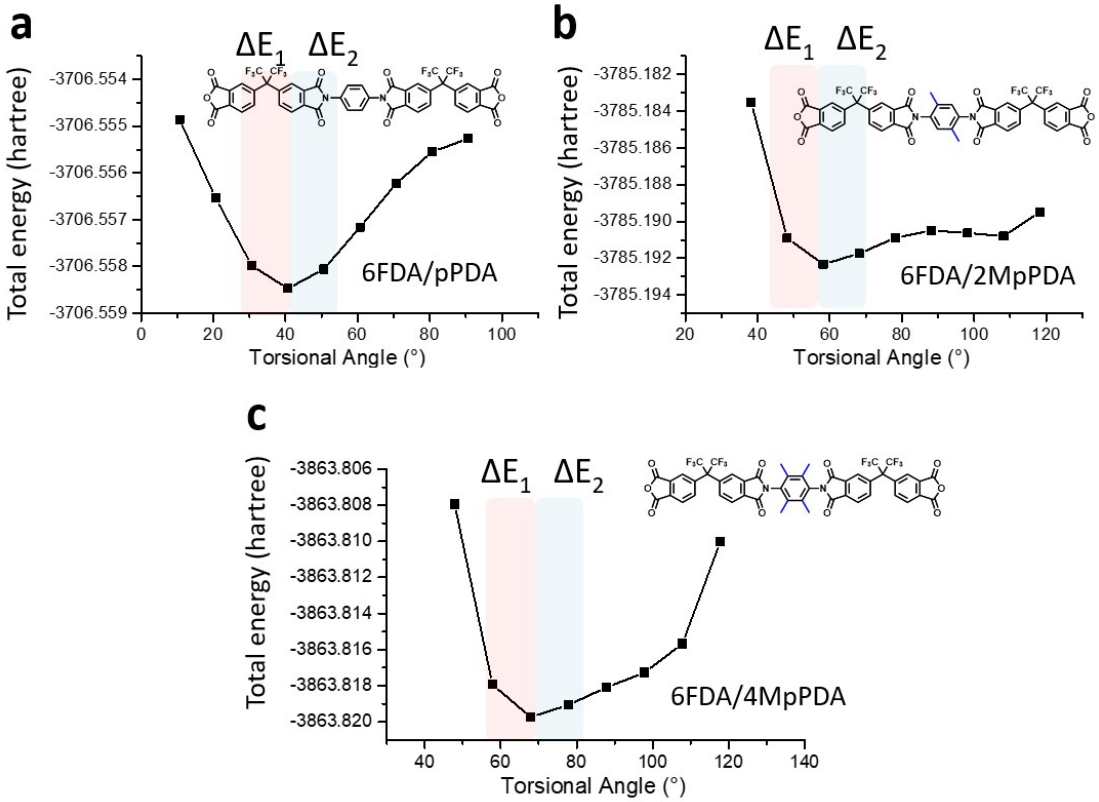

Fig S3 Energy variation of torsional angle φ2 in substituted pPDA series PI structures.

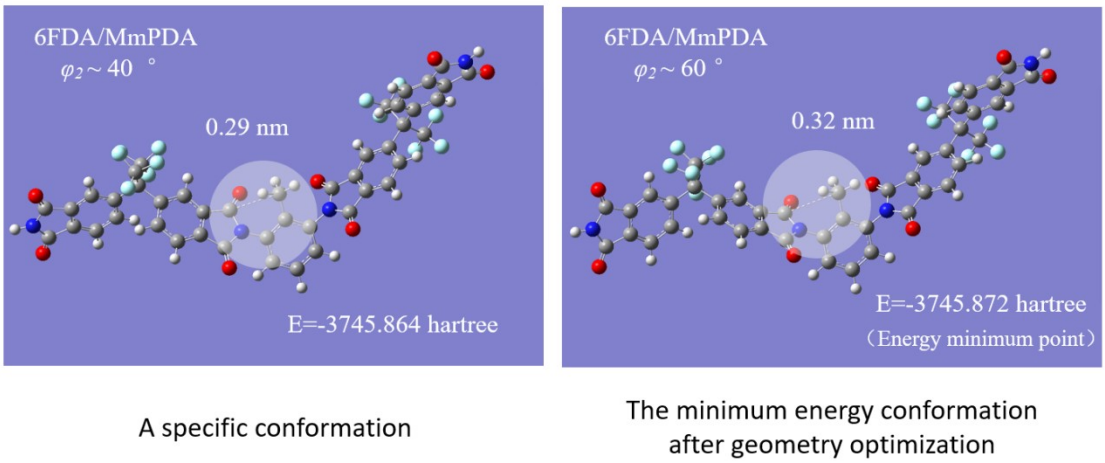

Fig S4 Particular conformation of torsional angle (6FDA/MmPDA as example).

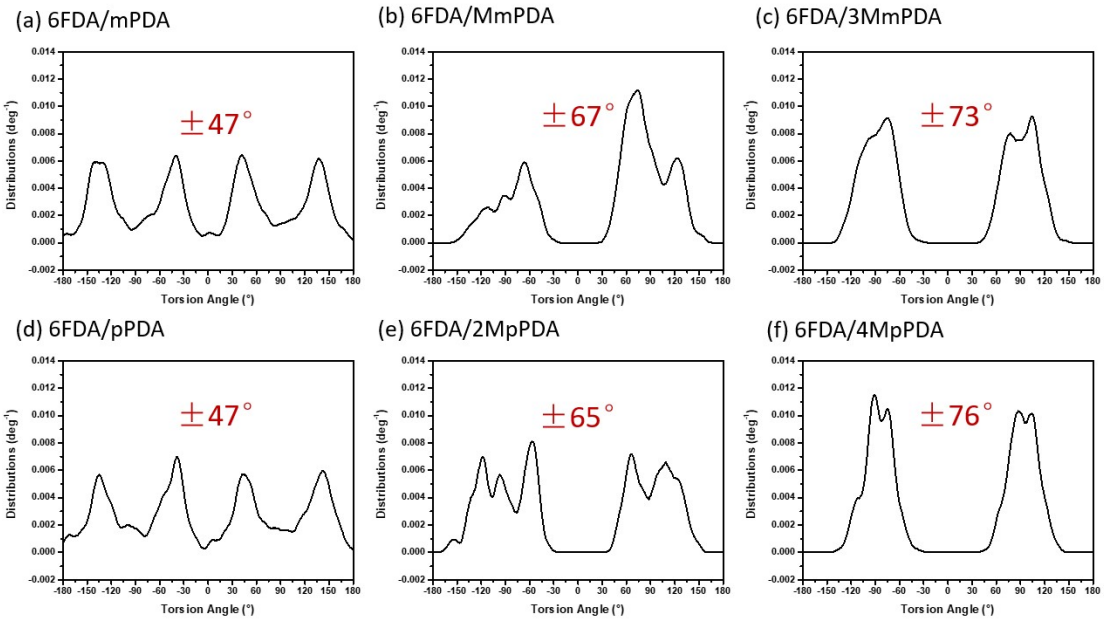

Fig S5 Distribution of torsional angle in amorphous PI cells. Calculation of the average torsional angle is described as following: searching the torsional angle in PI cells by Forcite module, the angle distributed from -180 ° to +180 ° are shown. Y axis stands for the frequency. Integrating the Angle with respect to Y gives the mathematical expectation, which is the average torsional angle. Specifically, the integration angle interval is from 0° to 90°, and the angle large than 90° or less than 0 ° is spatially equivalent to the small angle after subtracting 90° (i.e., 120 and 60 are equivalent).

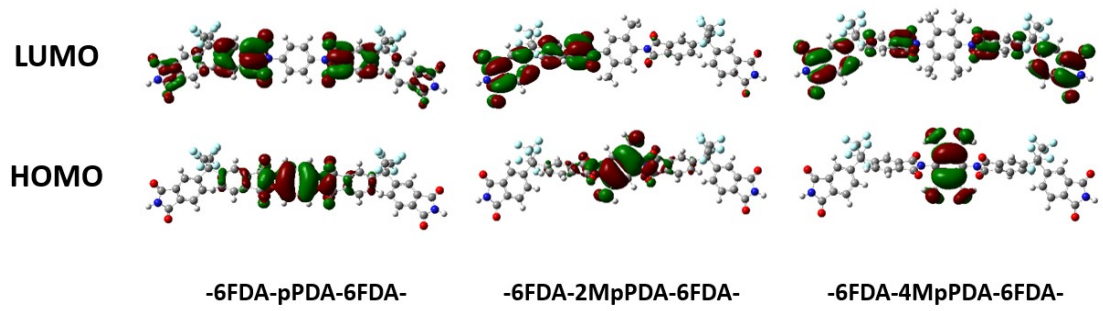

Fig S6 Molecular orbital (MO) diagrams of the substituted pPDA series polyimide.

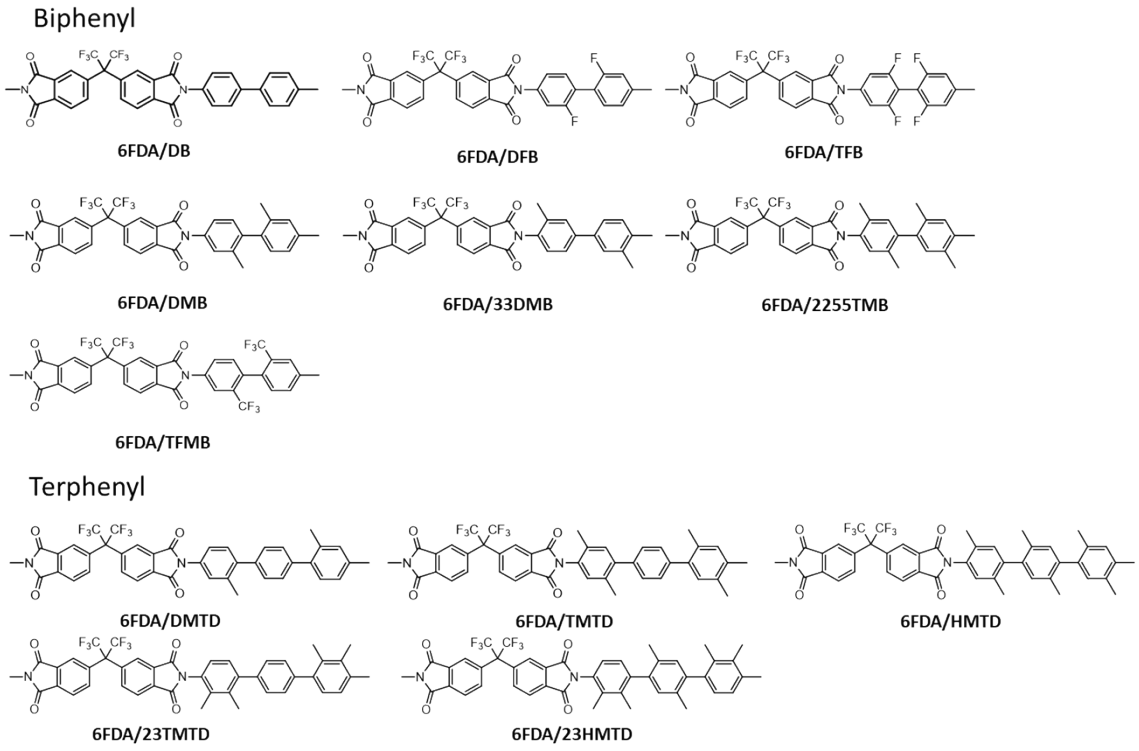

Fig S7 Chemical structures of previous reported PI structures.

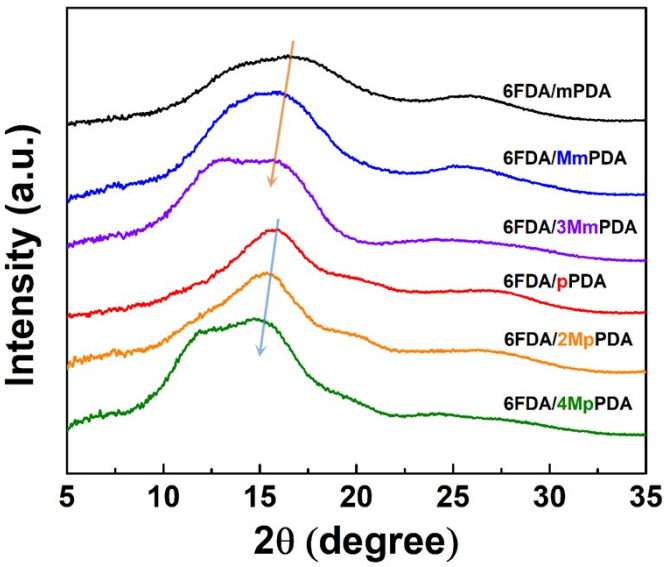

Fig S8 1D WAXD curves of CPI films.

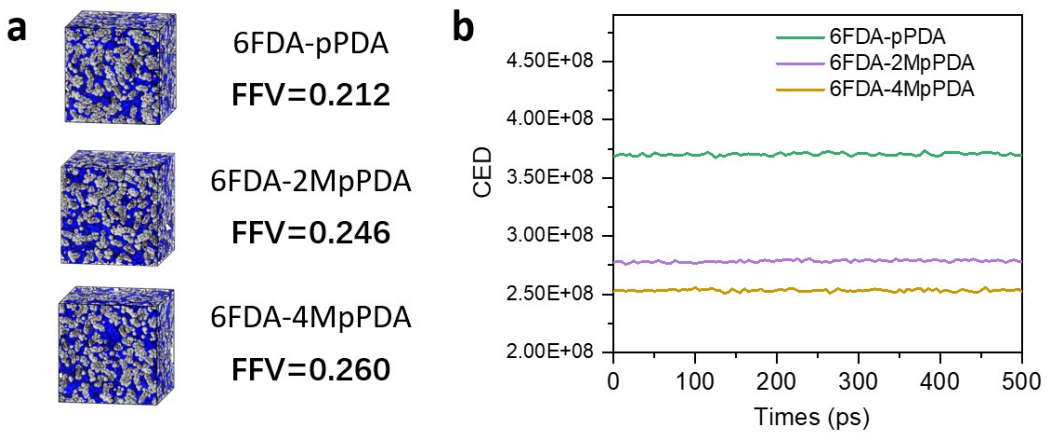

Fig S9 FFV and CED of amorphous PI cells.

2. Supplementary Table

Table S1 Thermal and mechanical properties of CPI films.

CPI films	T_g (°C)[a]	CTE (ppm/K)[a]	Fracture strength (MPa)	Initial modulus (GPa)	Elongation at break (%)
6FDA/mPDA	319	49.3	73±5	2.3±0.2	3.9±0.2
6FDA/MmPDA	368	46.0	60±4	2.7±0.2	2.4±0.1
6FDA/3MmPDA	407	52.0	74±4	1.9±0.1	6.8±0.5
6FDA/pPDA	374	48.3	96±7	2.5±0.2	6.1±0.4
6FDA/2MpPDA	388	44.8	82±6	3.3±0.2	3.5±0.2
6FDA/4MpPDA	409	40.8	81±4	2.3±0.1	9.5±0.7

a. Thermal expansion coefficient recorded using TMA from 50-250 °C.

Table S2 Energy barriers of the studied torsional angles

Samples	**ΔE_1 (hartree)**	**ΔE_2 (hartree)**	**Samples**	**ΔE_1 (hartree)**	**ΔE_2 (hartree)**	**Samples**	**ΔE_1 (hartree)**	**ΔE_2 (hartree)**
6FDA-mPDA	0.000524	0.000407	6FDA-MmPDA	0.001239	0.000512	6FDA-3MmPDA	0.001833	0.000633
6FDA-pPDA	0.000493	0.000415	6FDA-2MpPDA	0.001428	0.000583	6FDA-4MpPDA	0.0018	0.000674

Table S3 Molecular planarity of different repeating units, including torsional angles, molecular planarity parameter (MPP) and span of deviation from plane (SDP).

CPI films	φ_1	φ_2	Repeat unit		Planarity of φ_2	
			MPP	SDP	MPP	SDP
6FDA/mPDA	72.0	40.8	1.08	4.68	0.49	1.95
6FDA/MmPDA	72.1	60.5	1.09	5.07	0.89	3.43
6FDA/3MmPDA	72.0	73.8	1.13	5.46	1.03	4.61
6FDA/pPDA	71.9	39.5	1.07	4.68	0.52	1.73
6FDA/2MpPDA	71.5	60.8	1.07	5.11	0.92	3.76
6FDA/4MpPDA	72.1	66.6	1.08	5.40	0.96	4.33

Table S4 Calculation of charge transfer, energy gap and properties of excited states.

CPI films	E_{HOMO}/eV	E_{LUMO}/eV	E_g (eV)	E_{ex} (eV)	λ_{ex} (nm)
6FDA/mPDA	-6.66	-2.73	3.93	4.03	307.7
6FDA/MmPDA	-6.90	-2.70	4.19	4.09	303.2
6FDA/3MmPDA	-6.77	-2.69	4.09	4.05	306.2
6FDA/pPDA	-6.50	-2.75	3.75	3.92	316.3
6FDA/2MpPDA	-6.67	-2.70	3.96	4.06	305.4
6FDA/4MpPDA	-6.46	-2.69	3.77	4.05	306.2

Table S5 Optical properties and DFT recalculated results of previous reported PI structures (Chemical structures see Fig. S7).

Compositon	Literatures' data		DFT recalculated results			
	λ_{cutoff} (nm)	T_{400} (%)	E_{HOMO} (eV)	E_{LUMO} (eV)	E_g (eV)	E_{ex} (eV)
6FDA/DB	361	14.5	-6.08	-2.69	3.39	3.77
6FDA/DFB	342	50.3	-6.22	-2.76	3.46	3.87
6FDA/TFB	335	63.1	-6.52	-2.85	3.67	4.04
6FDA/DMB	342	44.1	-6.42	-2.67	3.75	3.89
6FDA/TFMB	322	80.2	-6.83	-2.83	4.00	4.06
6FDA/33DMB	338	66.0	-6.09	-2.66	3.43	3.92
6FDA/2255TMB	308	82.0	-6.25	-2.65	3.60	3.99
6FDA/DMTD	349.0	30.0	-5.96	-2.67	3.29	3.78
6FDA/TMTD	318.0	73.0	-5.93	-2.65	3.28	3.93
6FDA/HMTD	305.0	81.0	-6.18	-0.10	3.53	3.98
6FDA/23TMTD	310.0	78.0	-6.01	-2.65	3.36	3.98
6FDA/23HMTD	305.0	81.0	-6.15	-2.65	3.50	4.02

The optical properties of these PI films (~20 μm) are reported in previous literatures. The DFT simulations towards these PI structures are all re-calculated at DFT/B3LYP/6-31g (d) level with Gaussian 16 package after geometry optimization. And the $E_{ex.}$ are calculated at TDDFT/CAM-B3LYP/6-311++g (d,p).

Table S6 WAXD results of CPI films.

CPI films	2θ (°)	*d*-spacing (Å)
6FDA/mPDA	15.9	5.57
6FDA/MmPDA	15.4	5.75
6FDA/3MmPDA	14.8	5.98
6FDA/pPDA	16.0	5.54
6FDA/2MpPDA	15.6	5.68
6FDA/4MpPDA	15.0	5.90